RELATIONSHIP OF HIERARCHICAL STRUCTURE TO MECHANICAL PROPERTIES

E. Baer *, A. Hiltner and D. Jarus

Department of Macromolecular Science, Center for Applied Polymer Research
Case Western Reserve University, Cleveland, OH 44106, U.S.A.

SUMMARY: The mechanical properties in complex systems are explained based on the hierarchical structures present in the system. Hierarchical structures designed for specific mechanical responses are best exemplified by examples from biology. Collagen, a main component in soft connective tissues, is organized into hierarchical structures in the form of tendons or intervertebral discs as examples. Understanding these structures is vital in relating the structures to the intended properties. This approach is also used to characterize organic/inorganic natural composites such as human bone, reindeer antler and nacre. Another example of a hierarchical structure in biology with excellent mechanical properties is that of cellulose, when organized into wood. The importance of hierarchical structures also applies to synthetic polymers for a clearer understanding of the structure-property relationships. Solid-state biaxially oriented polypropylene has excellent tensile and impact properties, which are explained by the hierarchical structure induced during the processing. Thermotropic liquid crystalline polymers develop a hierarchical structure during injection molding that influence the final properties. Furthermore, the impact modification of polycarbonate is more easily understood when the system is explained in a hierarchical manner. It is also now possible to create or force hierarchical structures in synthetic polymers by microlayering technology. Several systems are outlined in which a hierarchical structure is created to enhance specific properties. SAN, a brittle polymer, can be microlayered with PC to create tough materials due to the scale, interaction and architecture of the microlayered composite. Another example is the effect of microlayered composite of PC/SAN on the interfacial adhesion mechanisms. Furthermore, toughening mechanisms in filled microlayers are examined based on the hierarchical structure .

INTRODUCTION

As the field of polymer science evolves, the polymeric systems developed are becoming increasingly more complex. However, the level of structural complexity is still less than that of natural occurring systems. Efforts toward systems that mimic complex and functionally designed natural materials are now in progress[1]. In understanding complex systems, the importance of treating the system on the molecular, nano-, micro- and macroscales has been proposed[2]. The structure-property relationships are best understood when the hierarchical nature of the system is taken into account. In the study of biocomposites, such as soft connective tissues, "three rules of complex assemblies" have been suggested[1].

 CCC 1022-1360/99/$ 17.50+.50/0

The first rule states that the structure of the composite is organized in discrete levels of scales. The minimum number of discrete levels, or scales, observed thus far in biocomposites is four. Virtually all biocomposite systems are bound to have distinct structural levels at the molecular, nanoscopic, microscopic, and macroscopic scales. The second rule states that the levels are held together by specific interactions between components. Whatever the nature of the bonding between levels, adequate adhesion is required to give the system structural integrity. Without this integrity, the composite system will not work. The third rule states that these highly interacting levels are organized into a hierarchical composite system that is designed to meet a complex spectrum of functional requirements that in some cases are adaptive.

This paper discusses examples from nature with complex hierarchical structure, and then gives examples showing how the hierarchical approach can aid the understanding of the mechanical properties of these systems. Subsequently, this approach is applied to explain the properties of complex synthetic polymer systems.

EXAMPLES FROM NATURE

Tendon

Tendon, a soft connective tissue between muscle and bone, is a classical hierarchical system. The structure of tendon is given[3] in Figure 1. The structure has six discrete scales of architecture. On the smallest scale, three polypeptide chains each coiled separately about a minor axis form a coiled coil around a single central axis. This triple helix is tropocollagen. Five tropocollagen units aggregate to form a microfibril[4]. Microfibrils are then joined into fibrils. The tropocollagen units are staggered along the length of the microfibril. This stagger results in the 64-nm banding seen in electron microscopy and x-ray diffraction evident on the fibril scale. These building blocks are what form the fascicle. It is at the fascicle level that the wavy crimp form of the tendon is evident. Note that at all levels of organization, the orientation is along the axis of the tendon. As the tendon is subjected to uniaxial tension almost exclusively, the structure is perfectly suited to uniaxial deformation. Uniaxial tensile curves of rat tail tendon as a function of age are given[3] in Figure 2. Except at the earliest ages, where the tendon is immature, four regions of behavior are evident. The initial toe region, which corresponds to the normal physiological loads, is the straightening of the crimped structure that occurs on the fibrillar level. The second region is the elastic stretching of the elements in the structural hierarchy. These regimes are reversible and no permanent damage occurs.

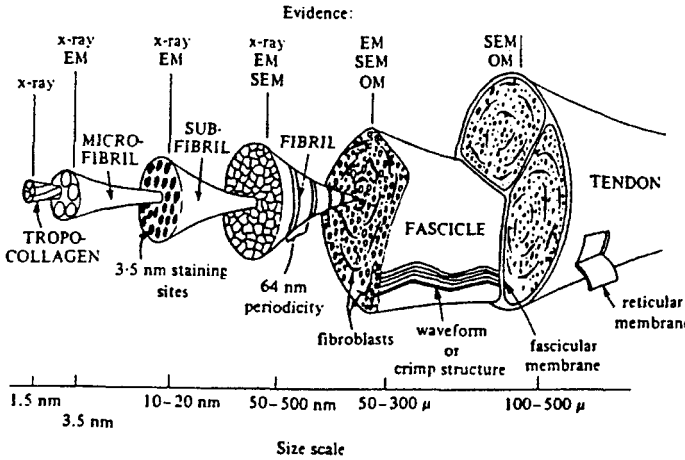

Figure 1 Hierarchical structure of tendon. Six discrete levels of organization are evident, ranging from tropocollagen at the molecular level to progressively larger and more complex structures at the nano- and microscales. The multilevel organization imparts the toughness of the tendon and, when exposed to excessive stress, individual elements at different levels of the structural hierarchy can fail independently. In this way, the elements absorb energy and protect the tendon as a whole from catastrophic failure.

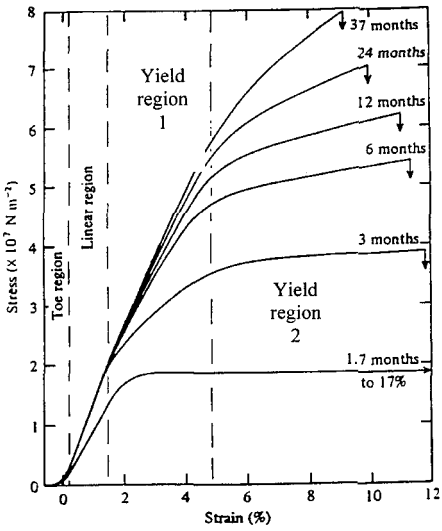

Figure 2
Stress-strain behavior of rat tail tendon. The stress-strain curve is divided into three regions. In the toe, the nonlinear behavior is the straightening of the crimp structure and corresponds to normal physiological loads. The linear region is elastic stretching of the straightened. This region of constant modulus extends until individual elements at the sub- and microfibrillar levels begin to break or slip in relation to one another. Differences in the hierarchical structure related to the age of tendon are manifested in all of these regions.

Removal of the load will result in complete recovery to the original crimped structure. The third (yield region 1) and fourth (yield region 2) are the onset of yielding and irreversible

damage. In the yield region 1, a small amount of band tilting occurs, indicating that damage occurs by shear-slip between microfibrils[3] (Figure 3).

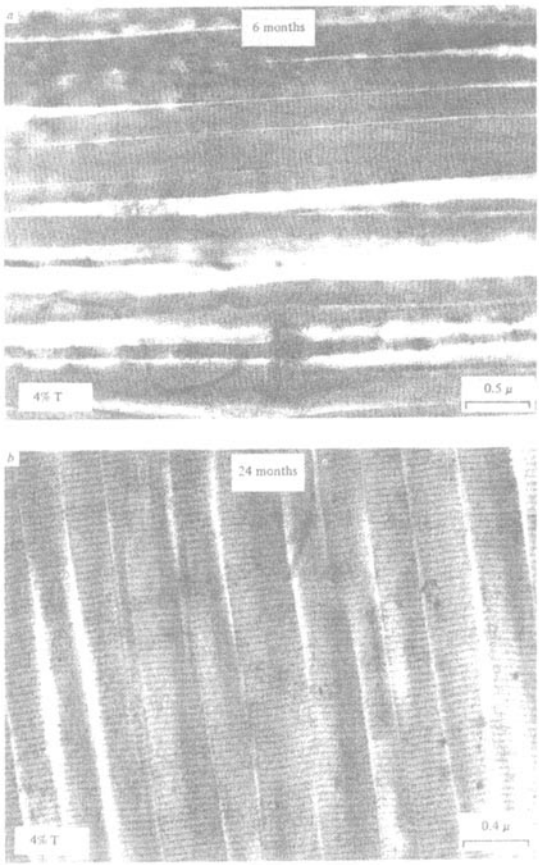

Figure 3
Electron micrographs of the tendon structure in yield region 1:
(a) 6-month specimen,
(b) 24-month specimen.
A small amount of band tilting occurs, indicating that the irreversible damage that occurs is caused by shear-slip between microfibrils. With increasing maturation, the hierarchical structure develops a resistance to shear-slip and less evidence of band tilting is seen.

This decreases with increasing age, as seen by the small change in modulus between the linear region and yield region 1. In the second yield region, severe band tilting occurs. Also, a loss of band contrast and the complete disappearance of banding occur. Shear-slip effects are reduced in this region and damage is confined to more localized sections that have dilated. Shredding of the fibrils is also evident as the fibrils fall apart laterally[3] (Figure 4). Damage in this region is incurred by slippage between the tropocollagen units with permanent dissociation on the fibrillar sub- and microscales. The multi-level organization of the tendon imparts the toughness shown. The failure of individual elements at different levels of the hierarchical structure absorbs energy and protects the tendon as a whole from catastrophic failure.

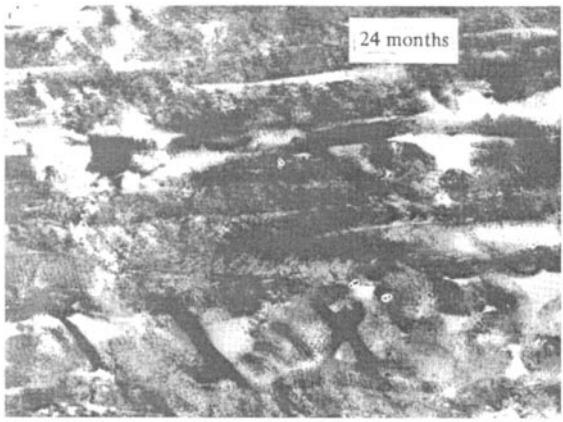

Figure 4
Electron micrographs of the tendon structure in yield region 2 of a 24-month specimen. Severe band tilting, a loss of the band contrast, and isolated fracture of the fibrils are shown.

Intestine

The intestine is composed of four distinct layers. Of these, the submucosa, composed of the majority of the collagen fibrils, is most responsible for the mechanical properties of the intestine. The hierarchical structure of intestine[5] is shown in Figure 5.

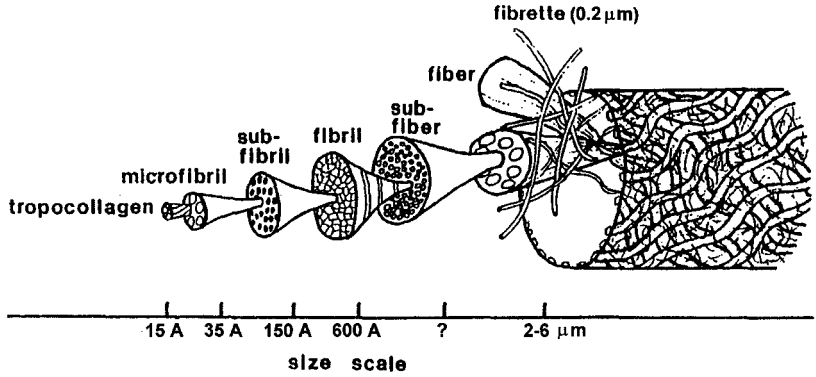

Figure 5 Hierarchical structure of the intestine. The hierarchical organization of the intestine is identical to that of the tendon from the molecular to the fibrillar level. The only difference is how the fibrils are arranged in the highest levels of the structure. No fascicles are present and, instead, the fibrils aggregate into fibers that are wound around the intestine in a helical fashion.

Note that the hierarchical structure is identical to that of the tendon through the fibrillar level. The only organizational difference is at the highest level of structure. The fibrils are oriented in layers biaxially around the intestine. The successive layers are at $\pm 60^{\circ}$ to one another, forming helices of opposite sense arrayed at $\pm 30^{\circ}$ to the longitudinal axis winding around the tendon. Furthermore, type III collagen is wound around the muscle wall as fibrettes, forming a

loosely woven mesh[6]. The mechanical properties of the intestine are derived primarily from the collagenous tissues. The hierarchical structure in the intestine is different from that of the tendon due to the different mechanical stresses incurred. The biaxial winding of the fibers prevents buckling of the intestine, while the multiple layers of helically wound fibers give maximum resistance to internal bursting. As with the tendon, the fibrils are planar crimped. The crimped morphology of the tendon in conjunction with the biaxial orientation of the fibers gives rise to anisotropic stress strain curves in tension[7] (Figure 6).

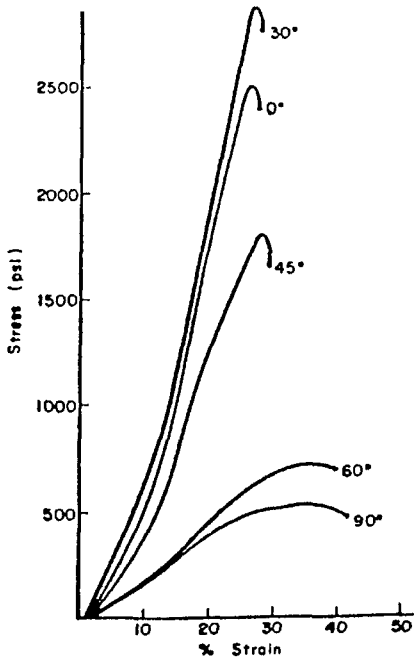

Figure 6
Stress-strain behavior of the intestine in tension. The tensile properties of the intestine vary with orientation, as would be expected of tissue made of biaxially oriented fibers. The intestine is stiffest with the least extensibility when stretched parallel to the fibers (30°) and longitudinally (0°). The greatest extensibility is seen perpendicular to the long axis (90°). These properties represent a structural adaptation to the functional demands of the intestine.

A toe region exists at low tensile strains with the removal of the crimped structure, followed by elastic stretching, and then irreversible deformation, similar to that of the tendon. In addition, fibrillar reorientation occurs within the layers to accommodate the deformation. The hierarchical organization is designed to provide the correct anisotropic mechanical properties. When the intestine is tested 30° to the longitudinal direction, the intestine is the stiffest due to the alignment with the fibers in one set of layers. Tested longitudinally, 0°, the intestine is only slightly less stiff. This prevents large changes of length in the intestine. Testing the intestine transverse to the longitudinal direction, 90°, the greatest extensibility is seen. Furthermore, once the crimp in the fibrils is straightened, the collagen fibers are strong and inextensible, which resists bursting.

Intervertebral disc

The intervertebral discs are interspersed between the vertebral bones in the spinal column. This hierarchical structure undergoes a complex form of loading being subjected to compressive loads caused by the weight of the body on the spine as well as torsion and bending loads during movement. The hierarchical structure designed for this complex loading pattern[8] is shown in Figure 7.

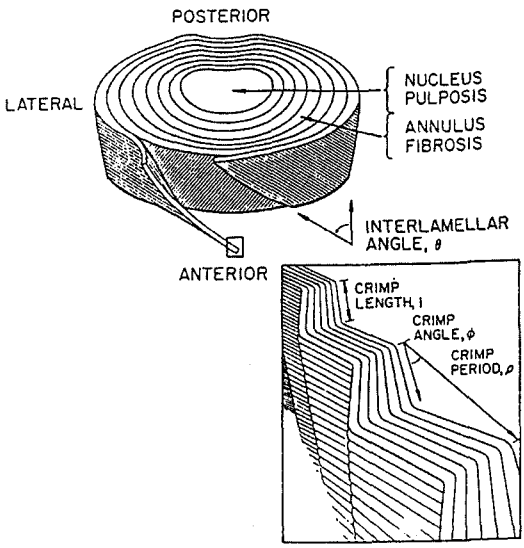

Figure 7

Hierarchical structure of the intervertebral disc. Collagen fibers are organized into lamellar sheets in the annulus fibrosus that surround a gelatinous and highly hydrated nucleus pulposus. The thickness of the lamellae vary with location and they are thicker at the anterior and lateral aspects of the disc than at the posterior. Within lamellae, the fibrils are inclined with respect to the axis of the spinal column by an interlamellar angle which alternates in successive lamellae. The orientation of the collagen fibrils in the annulus gives the disc strength and stability in tension, bending and torsional motions.

The disc consists of two sections. The center is the nucleus pulposis, which is a gelatinous matrix of proteoglycan molecules, fine fibers of type II collagen, and up to 88 % water[9]. The outer section is the annulus fibrosis, a structure of concentric cylindrical layers arrayed around the nucleus like the layers of an onion skin. These layers consist of lamellae of type I collagen fibers inclined with respect to the spinal axis by the interlamellar angle. The angle alternates with each successive layer, and varies with radial distance from the edge, ± 62° to ± 45° near the nucleus. The fibers in these layers have the same crimped structure like those of tendon; however, the crimp angle varies like that of the interlamellar angle, being 22° near the edge and 42° near the nucleus[8]. This gradient hierarchical structure utilizes the superior tensile properties of the collagen fibers in resisting the compressive forces oriented along the spinal axis as well as the torsional and bending forces. Examination of the discs fixed under compression reveals that as the disc is compressed, the nucleus pulposus spreads outward laterally, bulging the annulus outward[10]. Because the fibers in the annulus are anchored to the

vertebral bone, this results in the tensile loading of the fibers. The stress-strain curves of the disc in compression are therefore similar to those of the tendon in tension, with toe, linear, and yield regions[10] (Figure 8).

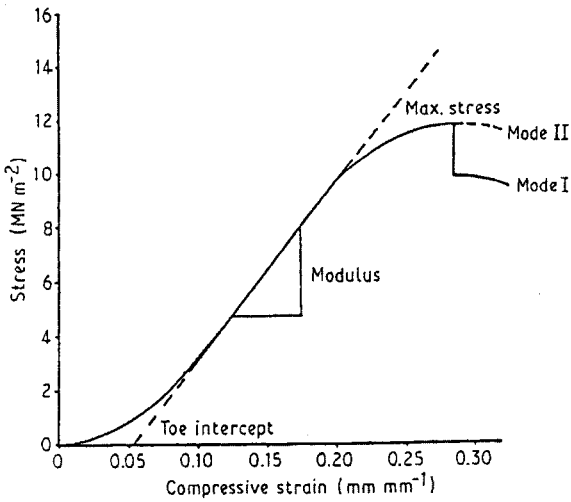

Figure 8
Compression stress-strain curves of intervertebral disc. In compression, the nucleus pulposus spreads outward laterally, bulging the annulus outward. Because the fibers in the annulus are anchored to the vertebral bone, this results in tensile loading of the fibers. The stress-strain curve is therefore very similar to that of the tendon in tension.

The biaxial organization of the layers also stabilizes the disc in torsion and bending. In torsion, the layers oriented in the direction of the twist are stretched in tension while the balance is unloaded. In bending, the biaxial lay-up prevents buckling of the fibers on the flexion side while resisting excessive bulging on the extension side.

In conjunction with the mechanical deformation of the disc is a transport issue. The time-dependent mechanical response of the disc is highly dependent upon the water content of the disc[11]. As this disc is compressed, water is squeezed out of the disc through the cartilage end plates that separate the disc from the vertebral bone. The stress relaxation and creep response of the disc under maintained compression are a result of the transport process. Creep and stress relaxation of the hierarchical structure can be modeled by considering a time- and strain-dependent hydrostatic pressure in the disc as water is squeezed out[11].

Nacre

A less complex biocomposite, which still shows excellent properties due to the interaction of the scaled architecture, is nacre (mother of pearl). Nacre exists to provide armor for various mollusks. Nacre consists of a lamellar structure of inorganic "bricks" composed of aragonite ($CaCO_3$) and a tough organic matrix that glues the aragonite together. The aragonite bricks

are 150-500 nm in thickness, with the organic adhesive being 20-200 nm in thickness[1]. The structure of nacre is depicted[1] in Figure 9.

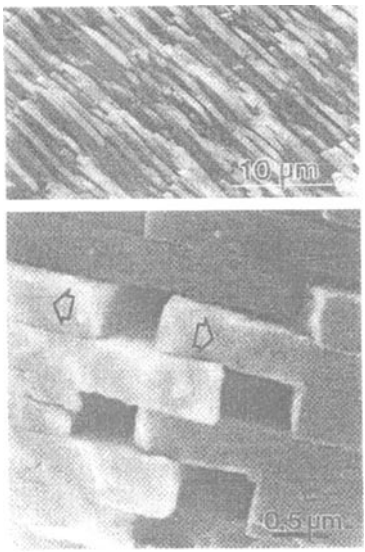

Figure 9
Structure of nacre. Aragonite bricks composing greater than 95 % the weight of the structure are held together by a thin organic matrix. The fracture mechanics imposed by this structure results in a fracture toughness that is several order of magnitude higher that that of monolithic aragonite. (Courtesy of M. Sarikaya)

The architecture of the nacre, in conjunction with the interaction of the organic and inorganic phases, allows the nacre to have fracture toughness values several orders of magnitude higher than that of monolithic aragonite. The flexural strength of nacre, between 100 and 200 MPa, is comparable to that of many common ceramics[12]. The complex micromechanics induced by the hierarchical structure of the mollusk are the cause of the large increases in toughness. Crack bridging, lateral pullout and sliding of the bricks, and crack arrest and branching are mainly responsible for the increase[13]. In fact, in bending, nacre does not often fail catastrophically but in a gradual fashion due to the tortuosity the crack follows due to crack branching in concert with the effects mentioned above. The fracture surface of *Strombus gigas* is shown[13] in Figure 10. Evidence of the tortuous nature of the crack path is clear.

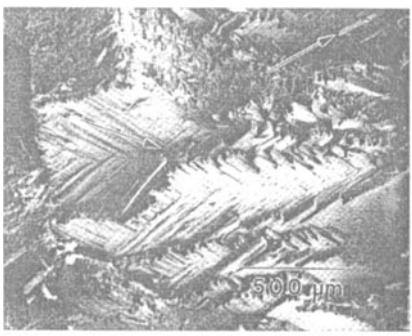

Figure 10
Fracture surface of *Strombus gigas*, a nacreous structure. The hierarchical structure of the nacre imposes a very tortuous fracture path, which results in a very high toughness.
(V. J. Laraia and A. H. Heuer[13])

Other examples of organic/inorganic composites exhibiting hierarchical structures in nature are reindeer antler and human bone. The high mineral content of antler with the specific structure allows for excellent impact properties. The hierarchical structure of antler is given in Figure 11.

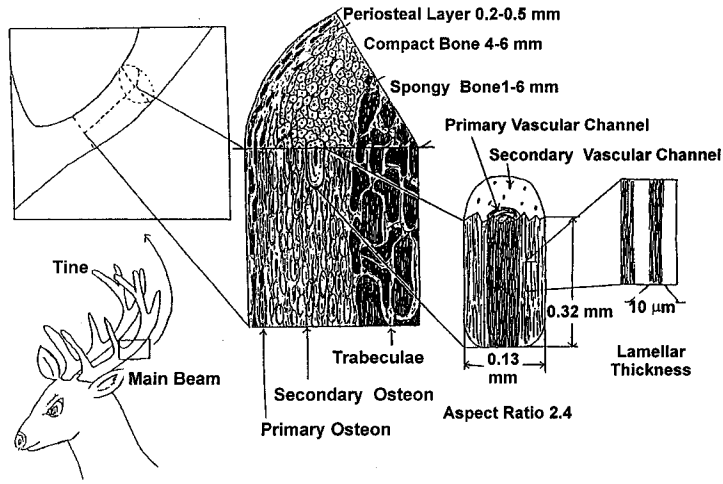

Figure 11 Hierarchical structure of reindeer antler. The gradient structure of the antler from the surface to the center decreases in mineral content and increases in porosity to meet both the mechanical and transport issues required of the antler. The osteons are composed of a circular lamellar morphology of collagen and hydroxyapatite.

Human bone, which is similar to antler but has an even more defined hierarchical structure due to the slower growth process, carries considerable loads and has excellent mechanical properties. Comparison of the structure of antler versus that of human femur is given[14] in Figure 12.

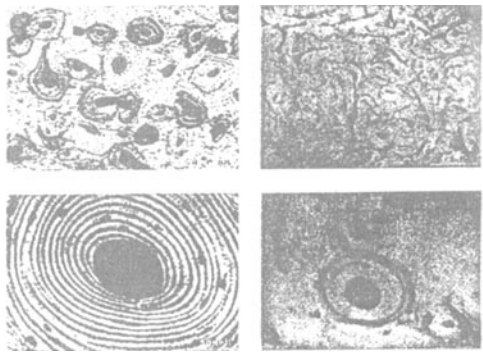

Figure 12
A comparison of the lamellar osteons of human femur and reindeer antler. The lamellar morphology of the femur, which develops more slowly, has much better defined morphology.

Wood

Examples of hierarchical structures in nature designed for their excellent mechanical properties are not limited to animals. Cellulose in wood is an excellent example of a very strong and tough material. The highly anisotropic mechanical properties of wood are shown in Figure 13 and can be explained by the hierarchical structure[15].

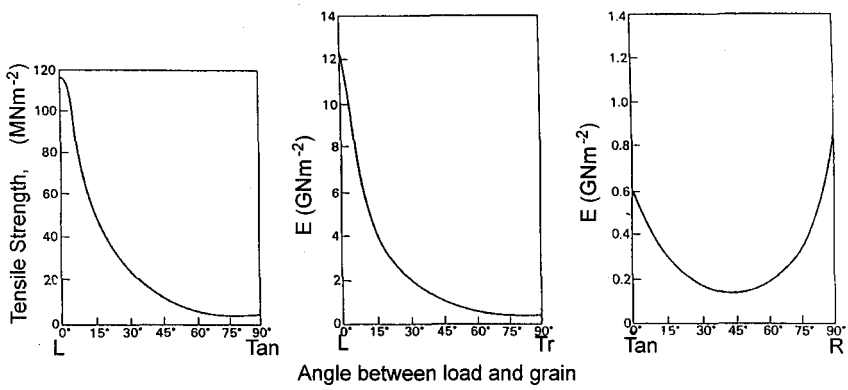

Figure 13 Tensile strength and modulus of wood tested across the three main axes of the tree. The highly oriented and hierarchical structure of wood results in highly anisotropic mechanical properties. (Reproduced from ref. 15.)

As is evident in Figure 13, the properties of wood are highly dependent upon the testing direction. In the longitudinal direction, the modulus and tensile strength are an order of magnitude higher than in the other orientations. The specific strength of wood can be four times that of steel. It is also of note that when hydrated, the fracture toughness of wood is excellent[1].

These highly tailored anisotropic properties of wood are due to the scale, interaction and architecture of the wood composite shown[1] in Figure 14. As with the tendon, organization and interaction of the components occurs on many scales, from the molecular organization to the macroscopic layered rings of the tree. The fracture toughness of wood is derived from the fracture mechanism imposed by the hierarchical structure. During fracture, the cellulose fiber wound cell wall will undergo helical column buckling. Interfibrillar cracks due to shearing will open and propagate longitudinally while the cylindrical wall collapses[15]. This allows each cell to be pulled apart rather than being broken in two. The similarity to the other hierarchical systems is of note. As with the tendon, failure can occur by shearing along the oriented axis on some scale, and the fracture path is very tortuous, similar to that of nacre. It is these common traits of the scale, interaction, and architecture in biological systems that

give the desired mechanical properties tailored for the specific loadings the natural system experiences.

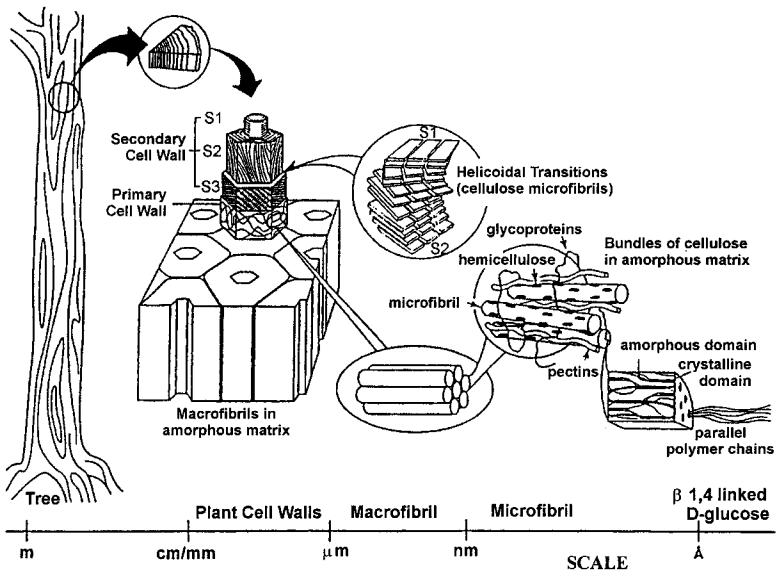

Figure 14 The hierarchical structure of cellulose in wood. The fracture toughness of wood when hydrated is excellent. This toughness is imparted by the hierarchical structure. (Courtesy of D. Kaplan)

SYNTHETIC POLYMER SYSTEMS

The lessons of biology on the complex hierarchical structures and the relationship to mechanical properties can be applied to synthetic systems for a clearer understanding of the mechanical properties of these systems. The development of hierarchical structures in synthetic polymers can be approached by several methods. Many attempts are being made by changing the chemistry of the macromolecule itself to form self-assembling systems[1]. Hierarchical structures can also be induced or changed by processing, and post-processing techniques. In general, the degree of hierarchy is less complex than that found in biological systems. Subsequently, an understanding of the properties of these systems using the hierarchical approach is feasible and simplified by understanding the lessons taught by nature.

Biaxially Oriented Polypropylene (PP)

The excellent mechanical properties of biaxially oriented polypropylene over those of unoriented PP can be derived from the manipulated hierarchical structure that is derived

during the post-processing in the solid state[16]. An extrusion process, which occurs at a few degrees below the melting point of PP, is used for the development of biaxially oriented PP sheet[17]. The engineering stress-strain curves of biaxially oriented PP at five different stages during the orientation process are shown[18] in Figure 15. The sample with the lowest amount of biaxial orientation had the lowest stress response and was deformed by necking. As the biaxial draw ratio was increased, homogeneous deformation occurred and the stress response of the system increased. The tensile impact strength of these samples is shown[18] in Figure 16.

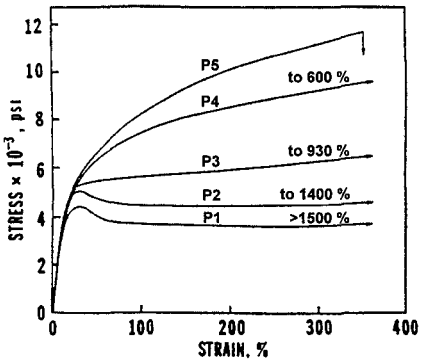

Figure 15
Stress-strain behavior of biaxially oriented polypropylene at different stages of the orientation process. An increased stress response with orientation is seen in conjunction with a change from yielding and necking to homogeneous deformation.

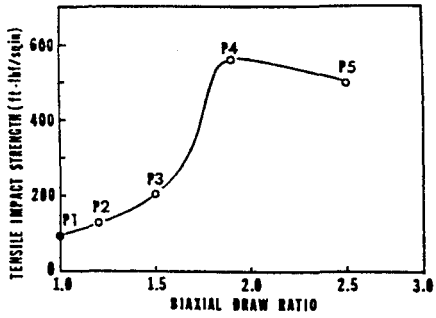

Figure 16
Tensile impact strength of biaxially oriented polypropylene at different stages of the orientation process. A large increase in the impact strength occurs between a biaxial draw ratio of 1.5 and 2. This was the same region where the tensile response changed to homogeneous deformation.

Note that the large increase in impact strength occurs at the biaxial draw ratio when homogeneous deformation occurs in the uniaxial tensile curves. On the microscopic scale, the deformation of the spherulites is shown for each position (Figure 17). In combination with SAXS and TEM data, the morphological changes in the structure are monitored. On the spherulitic scale, affine deformation of the spherulites into pancake-like disc structures is observed, and on the crystallite scale, lamellar rotation into the plane of deformation occurs until the biaxial draw ratio of 1.5 x 1.5. After this draw ratio, breakup occurs into smaller crystalline blocks. On the molecular scale, the b* axis gradually orients perpendicular to the plane, probably by a simultaneous tilting and shearing mechanism and the c-axis orients in the plane as a result of lamellar breakup. The amorphous chains are also preferentially oriented

in the plane. All of the planar-oriented polymer chains are located in two cone-like regions with the apexes joining at the center of the flattened spherulite[19].

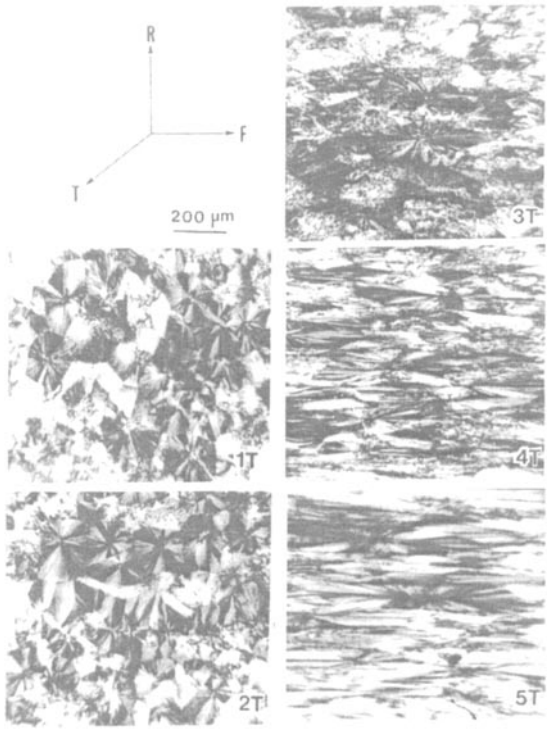

Figure 17
Optical micrographs of the spherulitic texture at different stages of the orientation process (transverse view). The spherulites are transformed into pancake-like disc shapes.

From these observations, the hierarchical structure shown in Figure 18 was developed.

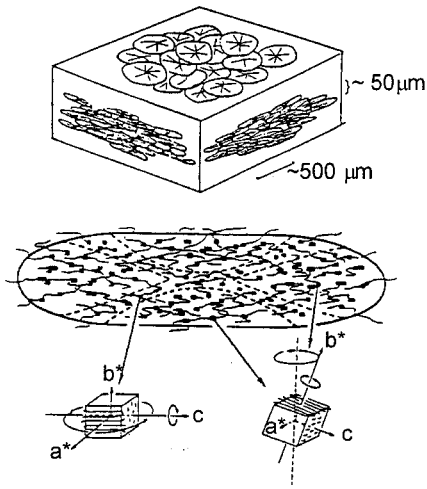

Figure 18
Hierarchical structure imposed by the biaxial orientation of polypropylene. Reorganization during the solid-state drawing process occurs on the micro (spherulitic) nano (crystallite) and molecular scales to impart a hierarchical structure with increased mechanical properties.

The large increase in the mechanical properties is a direct correlation with the development of the hierarchical structure that occurs at a biaxial draw ratio of 1.5 x 1.5. By understanding the oriented architecture on each scale in conjunction with interactions between scales, the large change in mechanical properties can be explained. The change in structure at a draw ratio of 1.5 x 1.5, which is reached between position P3 and P4, correlates with the change to homogeneous deformation with increased stress response in uniaxial tension, and the dramatic increase in tensile impact properties.

Thermotropic Liquid Crystalline Polymer (LCP)

Another example of a hierarchical structure induced by processing is the injection molding of a thermotropic LCP. The hierarchical structure is shown[20] in Figure 19.

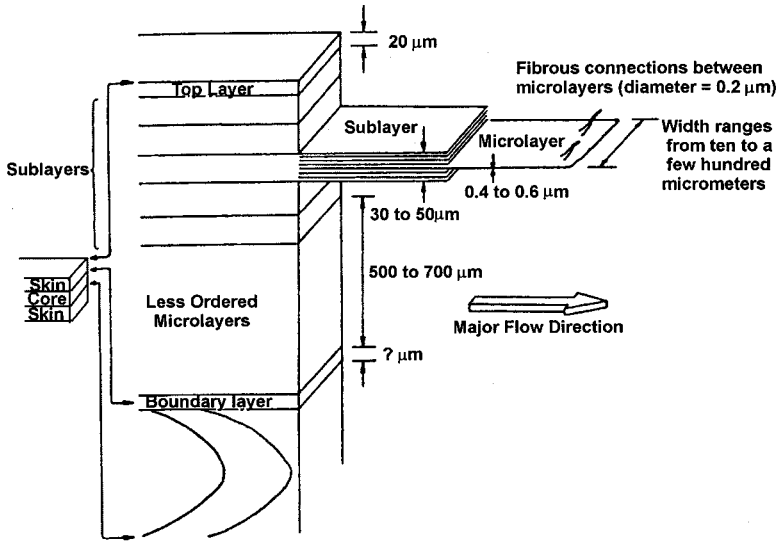

Figure 19 Hierarchical structure of a thermotropic LCP produced during injection molding. A gradient structure composed of sublayers, with microlayers inside each sublayer, creates a hierarchical structure. Fibrous connections between microlayers provide the integrity (interaction) of the system.

Macroscopically, the molding takes on the skin-core structure common to injection molding. The skin is also composed of sublayers, 30 to 50 μm thick. The next scale of architecture is actual microlayers 0.4 to 0.6 μm thick, which are connected by fibers 0.2 μm thick. The layered and oriented structure of the LCP has very anisotropic properties, analogous to that of wood. In fact, the LCP in the oriented skin layers fractures in a nature similar to that of wood[20] (Figure 20).

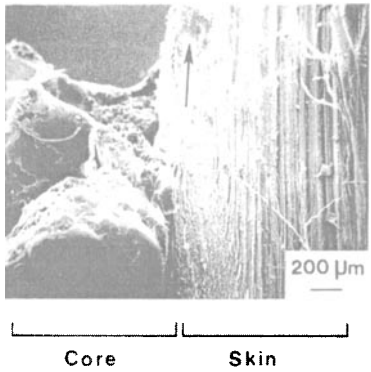

Figure 20

Fracture surface of an injection-molded thermotropic LCP. The oriented fibrous hierarchical structure of the LCP fractures in a manner similar to that of wood due to the similarities in their hierarchical structure.

Impact-Modified Polycarbonate

Hierarchical structures are also developed in the actual deformation of certain heterogeneous systems. If the scaling is correct, interactions between the components of the heterogeneous structure can develop which can be explained in hierarchical terms. In impact-modified polycarbonate, cooperative interactions of the impact modifier are a direct function of the impact-modifier loading[21]. The result is cooperative cavitation, shown as a function of loading in Figure 21. Random cavitation occurs at a loading of 2 %. As the loading is increased to 5 %, the beginning of arrays of cavitated particles is seen and is clearly evident at a loading of 10 %. The length of the cavitated arrays also increases with particle loading[21].

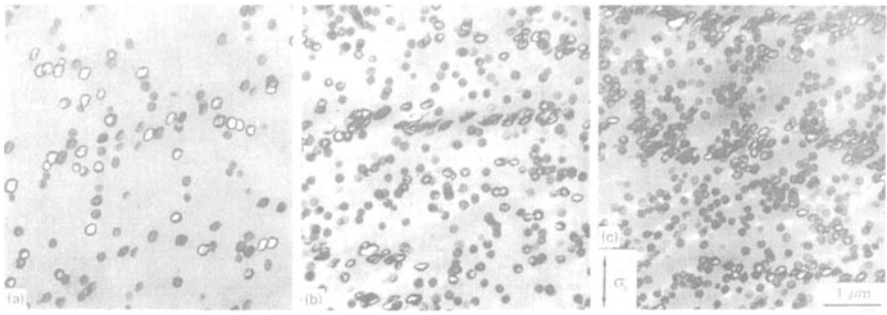

Figure 21 Electron micrographs of impact-modified PC as a function of impact-modifier loading. (a) 2 %, (b) 5 %, (c) 10 %. The increase in loading creates the correct scaling to allow for cooperative cavitation. At high loadings, arrays of cavitated particles exist which are due to the cooperative nature of the cavitation process.

The development of these arrays is caused by the impingement of a plastic zone formed during the cavitation of a particle with the nearest particle. The scaling between particles controls the cooperative interaction of the particles. A schematic of this cooperative effect is shown[21] in Figure 22.

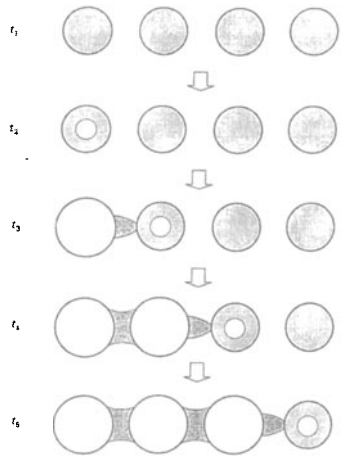

Figure 22
Schematic representation of the cooperative effect of cavitation caused by the elastic stress field present that overlaps with the next particle.

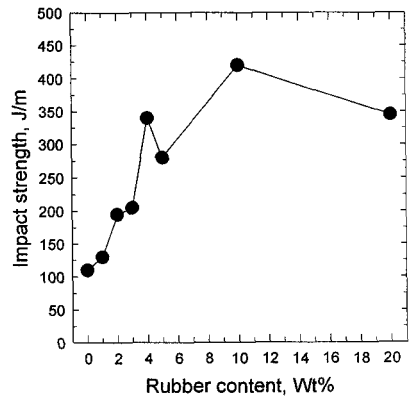

Figure 23
Impact strength of impact-modified polycarbonate as a function of modifier loading at – 40 °C. The impact values are highest at the loadings where the scaling between particles allows for cooperative cavitation and promotion of shear yielding in the matrix.

Particle-particle interactions that facilitate cavitation and promote matrix shear deformation are highly desirable for good low-temperature impact properties. The impact strength of impact-modified PC as a function of modifier loading at –40 °C is shown[21] in Figure 23.

A schematic of the effect of scaled interactions of the impact modifier with loading is shown[22] in Figure 24. The macro-, micro- and nanoscale deformation is altered by the change in micromechanics as the level of modifier is increased from 2 to 10 % because scaling controls the interactions between particles.

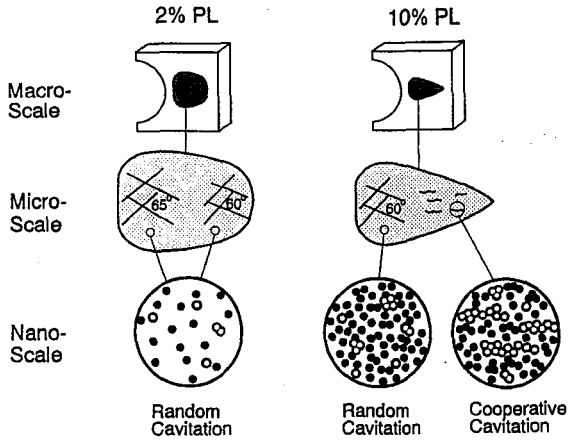

Figure 24
Schematic representation of the effect of scaled interaction of the impact modifier at different levels of the structure. The deformation is affected on each scale due to the cooperative cavitation.

POLYMER MICROLAYERS

In nature, the system has evolved to create an optimum structure for the required mechanical needs and functions. In most synthetic blends and composites, the hierarchical structure is most often created accidentally during the synthesis or processing of the polymer. Though there is continued effort to synthesize polymers which are more complex and self-assemble into hierarchical structures, processing routes exist today to control the structure down to the micro- and nanoscales[23,24]. The repeated existence of layered structures in biological systems stimulates the desire to develop synthetic polymer microlayers. The technique of coextrusion has been extended to create composites with thousands of layers by controlling layer thicknesses down to the nanoscale. As with the other systems, the properties of these complex composites can be best understood by examining the scale, interaction and architecture of the systems.

Polycarbonate (PC) - Styrene - Acrylonitrile (SAN) Microlayer Polymers

Composite microlayers of PC/SAN have been studied extensively[25-29]. Changing the composition or the number of layers while maintaining the same sheet thickness can vary the layer thicknesses in the composites. The uniaxial tension curves of 65/35 PC/SAN composites as a function of number of layers are shown[25] in Figure 25.

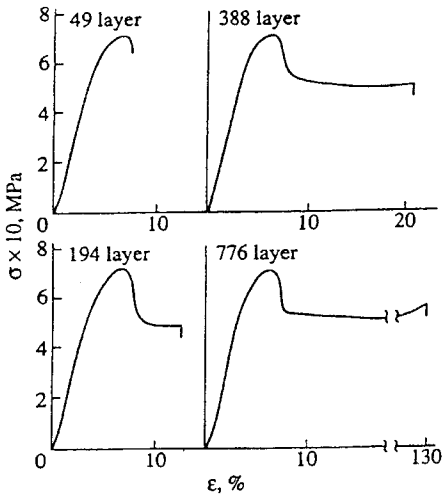

Figure 25
Uniaxial tensile curves of 65/35 PC/SAN microlayer composites as a function of layer thickness (constant thickness with increasing number of layers). Even though SAN is a brittle polymer, the composites show ductile behavior and the ductility increases as the layer thicknesses are decreased.

The layer thickness decreased from 30 to 2 μm as the number of layers was increased. Even though SAN is a brittle polymer, the composites showed ductile behavior, and the amount of ductility increased as the layer thickness was decreased. A micrograph of the irreversible deformation mechanisms for a given composite is shown[26] in Figure 26.

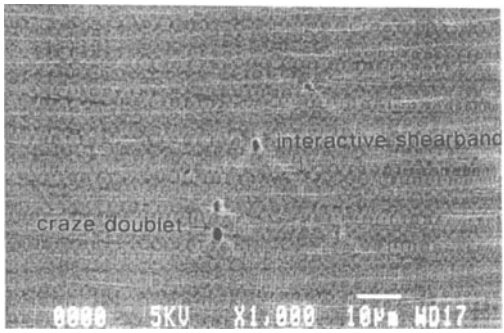

Figure 26
Optical micrograph of the microdeformation of PC/SAN microlayer. Cooperative crazing is evident in the form of a craze doublet, as well as interactive shear banding. The cooperative interaction, as the layer thickness decreases, changes the deformation mechanism in the SAN layers at the yield instability from craze opening to shear yielding.

The interaction between the layers is evident, and shear banding and crazing interact cooperatively as the layer thicknesses are decreased. Cooperative cavitation of SAN crazing is a function of the PC layer thickness. As the PC layer thickness is lowered, the plastic zone and subsequent elastic stress concentration at the craze tip into the PC layer can extend to the neighboring SAN layer[27] (Figure 27).

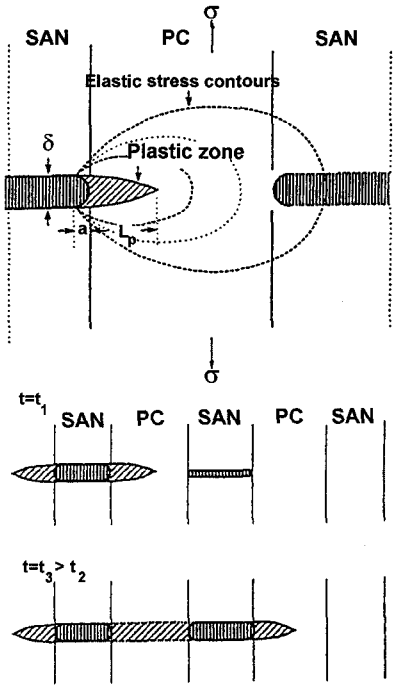

Figure 27
Schematic representation of the cooperative craze development and propagation in the microlayers.

This leads to craze doublets and, as the PC layer thickness is further decreased, to craze arrays[27] (Figure 28).

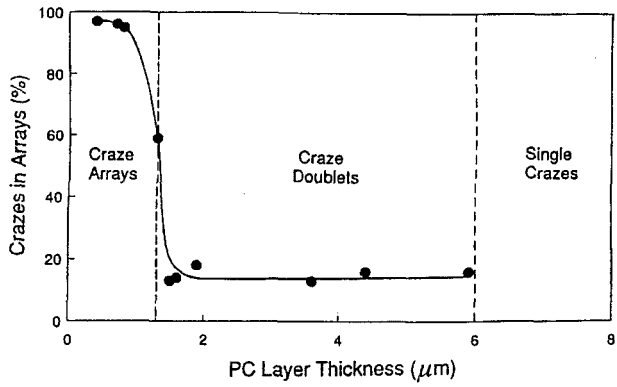

Figure 28 Total amount of crazes that are behaving in a cooperative manner as a function of PC layer thickness. As the layer thickness is decreased, cooperative crazing occurs as craze doublets. Below 1.5 μm, almost all crazes are in craze arrays.

This cooperative cavitation is very analogous to the cooperative cavitation of impact-modified PC. The PC layer also serves to blunt the craze by the formation of a shearband, so that a critical size void is not formed[25]. As the strain is increased, the microshear bands grow through the PC layers and extend into several adjacent SAN and PC layers. The cooperative behavior changes the deformation mechanism in the SAN layers at the yield instability from craze opening to shear yielding. The importance of scale and interaction in the layers is paramount. Changing the layer thickness to incorporate the correct scale and thus to allow for the synergistic interaction of the layers gives cooperative microdeformation mechanisms that prevent brittle fracture.

Microlayer Adhesion (PC/SAN)

The effect of the layer thicknesses in PC/SAN microlayer composites also affects the measured adhesion. Peel curves of different types of PC/SAN composites are shown[27] in Figure 29. The delamination toughness changes drastically as the layer thicknesses of the PC and SAN are varied. As with the tensile experiments, the micromechanics of the microlayer composite are crucial in understanding the delamination toughness. Micrographs of two different crack tips are given[28] in Figure 30. The method of delamination can involve crazing of the SAN layer ahead of the crack tip and the crack can also run along a single interface or several PC/SAN interfaces.

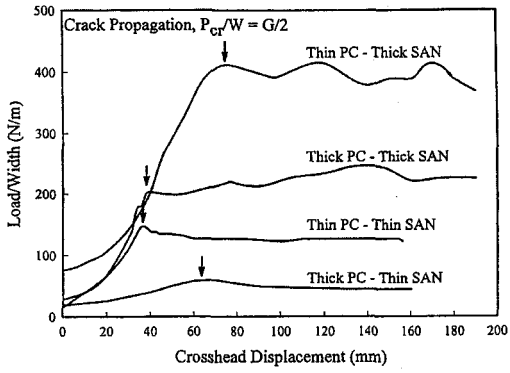

Figure 29
Peel curves of PC/SAN microlayers as a function of the combinations of layer thicknesses. Peel forces are a strong function of the layer thicknesses of each component.

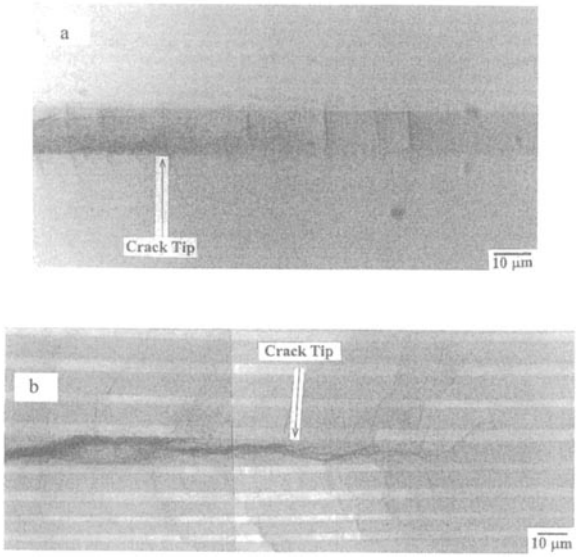

Figure 30
Crack tips of PC/SAN peel specimens showing effect of layer thickness on crack propagation. (a) Thin PC/ thick SAN. Crazing of the SAN occurs ahead of the crack tip and the crack runs along several different layers. (b) Thick PC/thick SAN. Crazing of the SAN layer occurs; however, the crack runs along a single layer.

Four different modes controlled by the layer thicknesses are summarized schematically in Figure 31 as single interface, multiple interface, single-layer craze, and multiple-layer craze delamination[28]. The PC layer thickness controls single- versus multiple-layer delamination, as the PC layer has to be thin enough for the stress at adjacent interfaces to initiate secondary cracks and also thin enough to tear easily. Crazing in the SAN layer is controlled by the SAN layer thickness. As the SAN layer thickness is decreased, a critical layer thickness of 1.5 μm is reached below which no crazing occurs. If the SAN layers are thick and the PC layers are thin, both mechanisms occurred with multiple-layer craze delamination. The effect of layer thickness on both the mechanism and G_{IC} of the peel specimens is shown[28] in Figure 32. Using thick PC layers and thin SAN layers, the actual interfacial delamination can be

measured without additional energy-absorbing mechanisms such as crazing or layer tearing to achieve a real measure of interfacial adhesion.

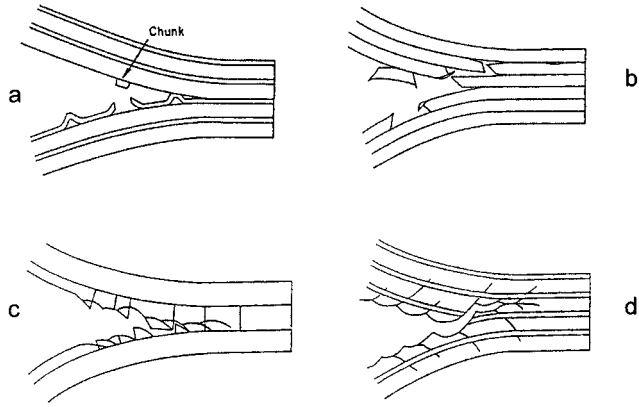

Figure 31 Schematic representation of the delamination mechanism as a function of layer thicknesses: (a) thick PC/thin SAN, (b) thin PC/thin SAN, (c) thick PC/thick SAN, (d) thin PC/ thick SAN.

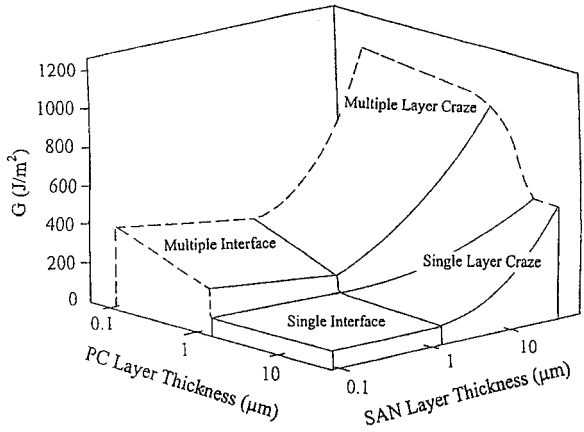

Figure 32
Map of the peel energies as a function of layer thickness and delamination mechanism.

Controlling the layer thickness allows the measurement of actual single interfacial delamination using thick PC and thin SAN layers. In all other cases, crazing or layer tearing provides additional energy-absorbing mechanisms and therefore the peel energies are much higher.

Talc-Filled PP

Microlayers of organic/inorganic composites also have very unique properties due to the scaled architecture and interactions imposed by the microlayering process. Composites of talc-filled polypropylene were made using the microlayer process. Examples of the talc-filled microlayer composites are given in Figure 33.

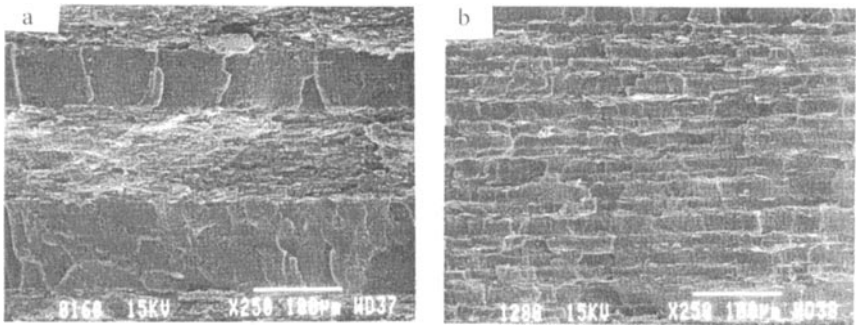

Figure 33 Microlayers of polypropylene and talc. Decreasing layer thickness aligns the talc particles better with the direction of flow. (a) 16 layers, (b) 128 layers.

The alignment of the talc particles by microlayer extrusion results in increased tensile modulus[29]. Furthermore, the alignment of the talc results in large increases in the fracture strain of the material[30] (Figure 34).

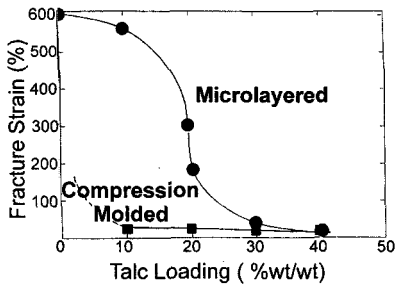

Figure 34
Comparison of compression molded and microlayered (PP/PP-talc) talc-filled PP as a function of talc loading. Ductility of the compression-molded samples is lost at 5-7 % loading, yet microlayers retain ductility until approximately 20 % loading. Crack blunting by the ductile PP layer in the PP/PP-talc microlayers inhibits crack growth and increases the fracture strain.

In comparison with compression-molded samples, where ductility is lost at 5-7 % loadings of talc, the microlayered samples remained ductile up to 20 % talc. In A-B samples, where the ductile PP layer could be expected to blunt cracks, analogous to the PC/SAN system with a ductile and a brittle layer, the effect of layer thickness was investigated. A peak in fracture strain occurred between 64 and 256 layers[30] (Figure 35).

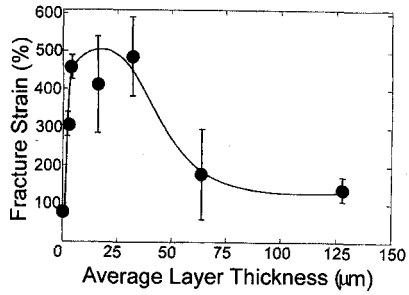

Figure 35
Fracture strain of PP/PP-talc microlayered composites as a function of layer thickness. Thick layers behave like bulk material and fracture at low strains. As the layer thickness is decreased, crack initiation and propagation in talc-filled layers is inhibited and blunted by the unfilled layers and critical size void cannot form. As the layer thickness is decreased further, particle agglomeration accelerates crack initiation and the ductile layers are too thin to blunt crack growth.

The scaling, interaction and architecture of the system can explain the change in ductility of the system. At low number of layers, the talc-filled layer behaves similar to that of a bulk sample, initiating a crack in the brittle talc-filled layer and forming a critical size void. Also, poor particle alignment results due to the large layer thickness with respect to the talc thickness. The poor alignment of the talc particles increases the probability of crack initiation. As the layer thickness is decreased, failure in the brittle filled talc layer is blunted by the ductile PP layer before a critical size void can be formed in conjunction with better aligned particles, resulting in the large increases in ductility. As the layer thickness is decreased further, the layer thickness approaches that of the talc particle itself. During the microlayer process, as the layers are cut and stacked thinner and thinner, the geometric constraint of the individual layers causes agglomeration of the talc particles. The particle agglomerates act as stress concentrators and significantly accelerate crack initiation. The inorganic filler also serves to increase the tortuosity of the crack path. A cryo-fractured surface of a talc-filled microlayer is shown in Figure 36. Note the similarity to the fracture surface of nacre.

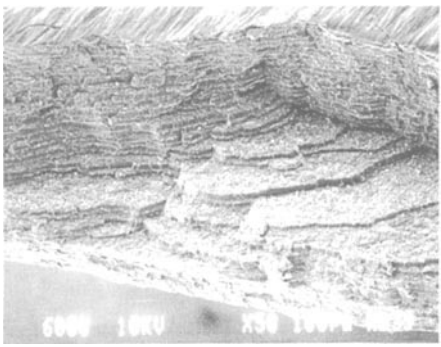

Figure 36
Cryofractured surface of PP/PP-talc microlayer. Note the similarity to the fracture surface of nacre. The filled and unfilled layers create a toughening mechanism by inducing a very tortuous crack path like that of nacre.

In summary, the importance of scale, interaction and architecture in structure-property relationships is paramount in the understanding of systems with ever-increasing complexity. The lessons that are available from biological systems with highly specialized architectures

designed specifically for mechanical and other multifunctional purposes are a guiding step in the development and understanding of complex systems.

Acknowledgements
The authors would like to thank the generous support of the Army Research Office (grant DAAG55-98-1-0311) and the National Science Foundation (grant DMR97-05696).

References

1 *Hierarchical Structures in Biology as Guide for New Materials Technology*, NMAB-464, Eds. I. A. Aksay, E. Baer, M. Sarikaya, and D. A. Tirrell, Washington, DC: National Academy, 1994
2 A. L. Bement, American Society for Metals and the Metallurgical Society Joint Distinguished Lecture in Materials and Society, Materials Week, October 1986
3 J. Kastelic and E. Bear, *Soc. Exp. Biol.*, 393 (1980)
4 J. W. Smith, *Nature*, 254, 157 (1968)
5 J. W. Orberg, L. Klein and A. Hiltner, *Connect. Tissue Res.*, 9, 187 (1982)
6 J. Anderson, Yaffe, and A. Hiltner, unpublished results
7 K. Fackler, L. Klein and A. Hiltner, *J. Microsc.*, 214, 305 (1981)
8 J. J. Cassidy, A. Hiltner and E. Baer, *Connect. Tissue Res.*, 23, 75 (1989)
9 P. Adams, D. R. Eyre and H. Muir, *Rheum. Rehab.*, 16, 22 (1977)
10 J. J. Cassidy, A. Hiltner and E. Baer, *J. Mater. Sci. Med.*, 1, 69 (1990)
11 J. J. Cassidy, M. S. Silverstein, A. Hiltner and E. Baer, *J. Mater. Sci. Med.*, 1, 81, (1990)
12 M. Sarikaya, J. Liu and I. A. Aksay, *Biomimetics Design and Processing of Materials*, 1995
13 V. J. Laraia and A. H. Heuer, *J. Am. Ceram. Soc.*, 72, 2177 (1989)
14 E. Baer and A. Hiltner, *J. Polym. Sci. Part A,* 38, 301 (1996)
15 *Mechanical Design in Organisms*, Ed. S. A. Wainwright, Princeton University Press (1976)
16 A. R. Austen, D. V. Humphries and C. L. Fay, *ANTEC Tech. Papers* (1982)
17 A. R. Austen and D. V. Humphries, U.S. Patent 4,282,277 (1981)
18 S. J. Pan, H. I. Tang, A. Hiltner and E. Baer, *Polym. Eng. Sci.*, 27, 869 (1987)
19 S. J. Pan, H. R. Brown, A. Hiltner and E. Baer, *Polym. Eng. Sci.*, 26, 997 (1986)
20 T. Weng, A. Hiltner and E. Baer, *J. Mater. Sci.*, 21, 744 (1986)
21 C. Cheng, A. Hiltner, E. Baer, P. R. Soskey and S. G. Mylonakis, *J. Mater. Sci*, 30, 587 (1995)
22 C. Cheng, A. Hiltner, E. Baer, P. R. Soskey and S. G. Mylonakis, *J. Appl. Polym. Sci.*, 55, 1691 (1995)
23 W. J. Schrenk, U.S. Patent 3,884,606 (1975)
24 W. J. Schrenk and T. Alfrey, Jr., *Polymer Blends*, Vol 2. (1978)
25 M. Ma, K. Vijayan, A. Hiltner, E. Baer and J. Im, *J. Mater. Sci.*, 25, 2039, (1990)
26 K. Sung, D. Haderski, A. Hiltner and E. Baer, *J. Appl. Polym. Sci*, 52, 147 (1994)
27 D. Haderski, K. Sung, J. Im, A. Hiltner and E. Baer, *J. Appl. Polym. Sci.*, 52, 121 (1994)
28 T. Ebeling, A. Hiltner and E. Baer, *J. Appl. Polym. Sci.*, 68, 793 (1998)
29 T. Ebeling, Ph.D. Thesis, Case Western Reserve University, 1998
30 C. Mueller, S. Nazarenko, T. Ebeling, T. Schuman, A. Hiltner and E. Baer, *Polym. Eng. Sci.*, 37, 355 (1997)